Asian Journal of Information Technology 5 (11): 1231-1238, 2006


# Brushless DC Motor with Asymetrical Magnetizing and Combination Control

Sameer H. Khader
Palestine Polytechnic University, P.O.Box 198, Hebron, Palestine

**Abstract:** This study describe the mathematical method applied for realizing optimized electromagnetic torque with reduced ripple in a two phase brushless dc motor with special rotor construction. The conventional construction of two-phase two-pulse brushless dc motor is inapplicable due to high torque ripples, Low mean torque and speed fluctuation, therefore a special rotor construction with aim to realize successful starting and ensuring relatively constant torque with minimized ripples and independent of the rotor position is going to be applied. In addition to introducing the modified rotor construction, a combined PWM control strategy and continuous control signal energized two-phase three-windings motor is applied. The produced electromagnetic torque by this approach is determined by applying Coenergy method and the numerically obtained results are going to be verified with experimental results. Good coincidence between both results is expected to be achieved.

**Key words:** DC Motors, synchronous motors, PWM, power electronics and induction machines

## INTRODUCTION

Unlike a conventional dc motor, brushless dc motor has an "inside-out" construction[1,2] , i.e., the field poles rotate and the armature is stationary. The field poles consist of permanent magnets mounted on the outside of the rotor surface and the armature is wound on a slotted or a salient pole laminated sheets. The armature coils are switched by transistors instead of the commutator. This arrangement has several advantages over small conventional DC motor or AC motor such as

- High efficiency
- Daptability for speed control
- High speed operation
- Long operation life and absent rotor losses in addition to the operation from low voltage dc supply.

Typical small-power applications in dc fans for cooling electronic equipments and closed spaces. Brushless dc motor fans are smaller in size and weight than ac fans using shaded pole or Universal motors.

These motors are able to work with the available 24 V or 12V dc supply and make them convenient for use in electronic equipment, computers, mobile equipment, vehicles and spindle drives for disk memories, because of it's high reliability, efficiency and ability to reverse rapidly. Brushless dc motors in the fractional horsepower range have been used in various types of actuators in advanced aircraft and satellite systems[3,4].

In addition to the developed electromagnetic torque and due to interaction between the armature current and the permanent magnet excitation, it is necessary to obtain an additional torque component, such as reluctance torque yield by the differences in magnetic permance in both quadrant and direct axis. Therefore, torque–null regions are eliminated[5,6].

## ANALYSIS

The motor analysis describes the following tasks.

**Motor windings and phase currents:** Brushless dc motors could be applied for various types of windings: single-phase/single pulse, two-phase/two pulses, three-phase three pulses and three-phase/six pulses motors.

The interest on two-phase brushless dc motor comes due to the simplicity of the driving circuit and the minimized total cost of the motor.

The elementary two-phase Brushless dc motor usually consists of permanent magnet rotor, stator with two windings spaced by 90° each other and drives by two power transistors controlled by control unit.

Each transistor is switched- on for 180°. The torque is produced by the interaction of the rotor magnetic field and the winding current nulls (each 180°). The presence of null points in electromagnetic torque is the main limitation for the widespread application because of the following several reasons:

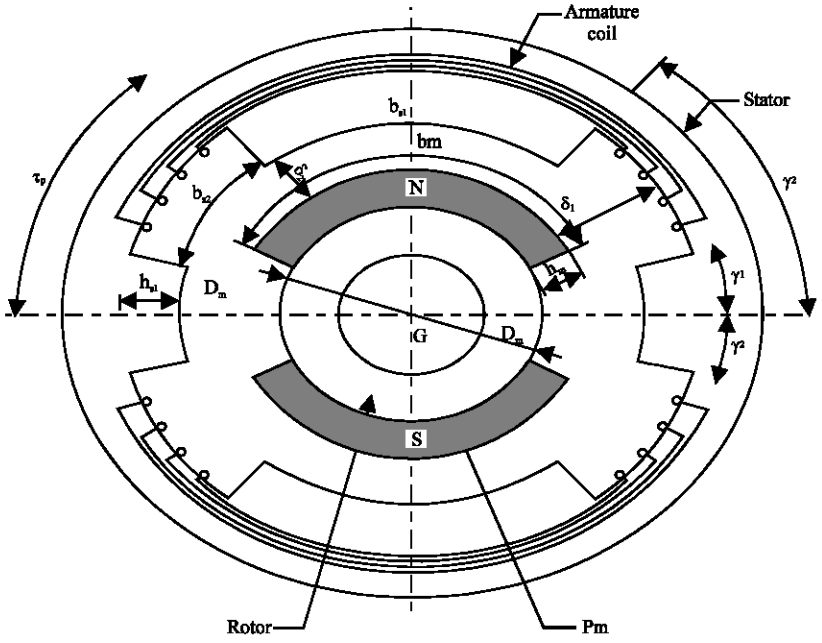


Fig. 1: Cross section from the motor construction

- First, the motor will not start from the null position,
- Second, high ripples in the electromagnetic torque, therefore the speed will fluctuate with rotor position and
- Third, high current at low speed and additional losses.

These drawbacks makes the motor impractical for commercial use unless one of the following solutions should be applied:

**Polyphase motor:** This motor has no torque nulls and characterized with relatively constant torque. This motor is not a subject of this study.

**Asymmetrical rotor construction (magnetization):** The rotor teeth are performed with predetermined high and width; this is made with purpose to obtain asymmetrical magnetic permance in the motor airgap. A partial cross section of such a motor construction is illustrated on Fig. 1, which is the subject of present study.

Figure 2 illustrates the distribution of the magnetic permance in the airgap decomposed in harmonic spectrum obtained by applying Fast Fourier Transform (FFT).

From these figures, it is shown that by introducing some asymmetries in the rotor construction, high orders of the magnetic harmonics are generated, producing an additional torque and therefore avoiding torque null points.

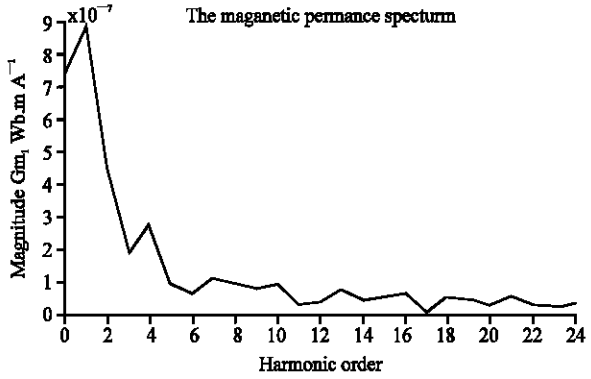


Fig. 2a: Harmonic spectrum of the magnetic permance in the airgap

Two torque components can be produced by applying this construction:

- An electromagnetic torque which form is expected to be sinusoidal positive change,
- A reluctance torque with nulls of the torque does not coincides with the nulls of the electromagnetic torque.

After avoiding the torque-null points in the motor, the torque-ripples issue should furthermore be reduced.

The torque ripples reduction could be achieved by applying various approaches, one of these is called "Combination Control". Hereinafter more details about this method.

**Combination control:** Regarding to Fig. 3, the motor coils (phases) are controlled as follow: S1 and S2 are energized continuously for half period each one, while the third coil S3 is energized by applying the PWM control for full period.

Figure 3b presents the time-switching diagram for both coils, where S3 must energized by pulse patterns for full period. Because of this control approach, S1 and S2 have large number of turns and concentrates on first half and second half of the stator periphery, while third coil S3 has less number of turns and uniformly is distributed in the stator periphery. This is made to obtain approximately sinusoidal flux distribution.

The following analytical modeling combines two solutions. Asymmetrical magnetization and combination control.

**Switching pulse generation:** Transistors T1 and T2 are switched continuously for 180°. Each one and connect the supply voltage to the coils S1 and S2 in complementary sequence. While transistors T3 and T4 switch the supply voltage to the third coil with polarity and time-duration determined by the applied PWM control strategy, as shown in Fig. 3b.

**Phase current calculation:** The motor phase current differs in coils S1,S2 and S3, where the current in the first two coils has a continuous character and approximately with constant value at a steady state operation, while the current in third coil is formed nearly to the sinusoidal waveform depending on the pulse PWM control strategy, induced back emf and on the magnetic permance.

**Phase current:** The phase current of $I_A(\alpha)$ in integral form is presented as follow:

$$\int_0^{\pi} di_A(\alpha) = \int_0^{\pi} \frac{U_{ds} - e_A(\alpha)}{L_A(\alpha)} d\alpha + \int_0^{\pi} \frac{R_A(\alpha).i_A(\alpha)}{L_A(\alpha)} d\alpha + \int_0^{\pi} \frac{i_A(\alpha)}{L_A(\alpha)} dL_A(\alpha) \quad (1)$$

The current in the second phase $I_B(\alpha)$ has the same shape.

The obtained results are displayed on Fig. 4 for both phases, where each phase operates 180° only. We observed that the phase current depends on the rotor position and coil parameters.

The coil current $I_C(\alpha)$ could be calculated taking into account the modulation function $h(\alpha)$ as described in[5]. The pulse duration of the generated train of pulses depends on the selected harmonics that must be eliminated. These harmonics are existed on the quarter wave interval from αmin to αmax.

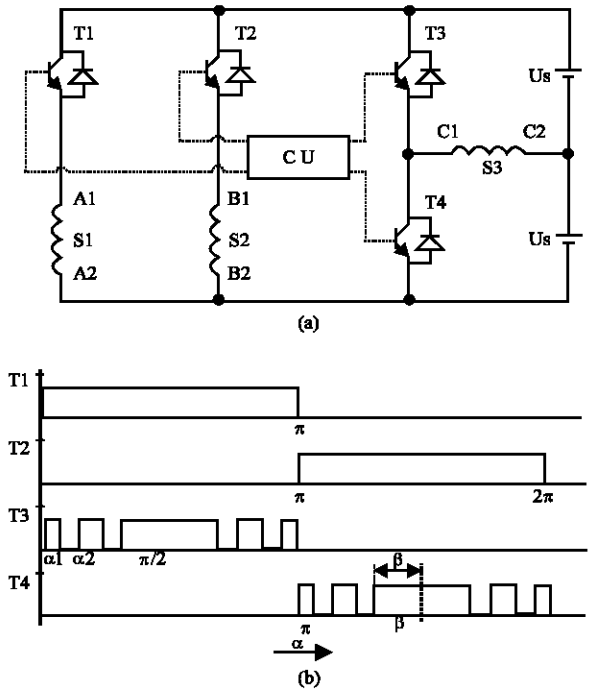


Fig. 3a: Electrical simplified circuit; b) generating of the PWM Pulse sequence

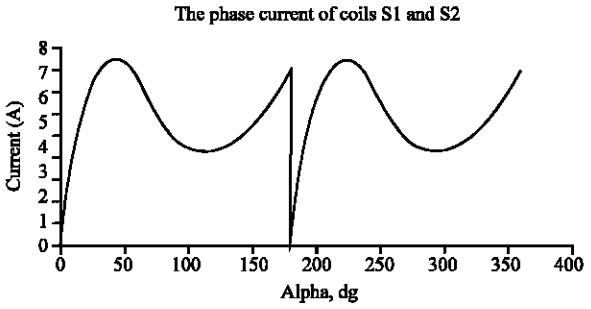


Fig. 4: Phase current of both coils S1 and S2 at speed of 1000 rpm

The Fourier series of the required odd quarter-wave signal could be presented by assuming the following harmonic function[5,6]:

$$h(\alpha) = \sum_{n=1}^{\infty} A_n \sin(n\alpha)$$
$$A_n = \frac{4}{n\pi} \sum_{k=1}^{N_p} (-1)^{k+1} \cos(n\alpha_k) \quad (2)$$

where Np- odd or even numbers, and

$$\alpha_{min} < \alpha_1 < \alpha_2 \ldots\ldots\ldots\ldots < \alpha_k < \pi/2.$$

Assuming that n1,n2,… …nNp are the harmonics that must be eliminated, the following set of algebraic equations is expressed:

$$\begin{aligned} 0 &= \sum_{k=1}^{\infty} (-1)^{k+1} \cos(n1\,\alpha k) \\ &\vdots \\ 0 &= \sum_{k=1}^{\infty} (-1)^{k+1} \cos(n_{Np}\,\alpha k) \end{aligned} \tag{3}$$

The obtained algebraic matrix is solved, producing a set of pulse patterns with switching instant αk and the voltage applied across the third coil S3 obtained for certain speed and frequency is presented on Fig. 5.

By applying the KVL and taking into account motor equivalent circuit with concentrated parameters, the balanced voltage equation for the third coil is:

$$\begin{aligned} &Ud = Us.h(\alpha) \\ &Ud = Rcic(\alpha) + \frac{d\lambda c(\alpha)}{d\alpha} + ec(\alpha) \\ &ec(\alpha) = Emc\sin(\alpha) \\ &\lambda c(\alpha) = Lc(\alpha).ic(\alpha) \end{aligned} \tag{4}$$

The leakage inductance depends on the rotor construction and its position and can be presented as follow:

$$Lc(\alpha) = Lo + \sum_{q=2,4,\ldots}^{\infty} Lmq\cos(q.\alpha) \tag{5}$$

Substituting Eq. (5) in Eq. (4), the voltage equation is expressed as follow:

$$Ud = ec(\alpha) + Rcic(\alpha) + Lc(\alpha)\frac{dic(\alpha)}{d\alpha} + ic(\alpha)\frac{dLc(\alpha)}{d\alpha} \tag{6}$$

By applying the principle of implicit integration, which form is present below:

$$\begin{aligned} \int_{\alpha 1}^{\alpha 2} dic(\alpha) &= \int_{\alpha 1}^{\alpha 2} \frac{Ud - ec(\alpha)}{Lc(\alpha)} d\alpha + \int_{\alpha 1}^{\alpha 2} \frac{Rc(\alpha)ic(\alpha)}{Lc(\alpha)} d\alpha \\ &+ \int_{\alpha 1}^{\alpha 2} \frac{ic(\alpha)}{Lc(\alpha)} dLc(\alpha) \end{aligned} \tag{7}$$

The results of solving Eq. 7 for various modulation index, modulation frequency and speed are graphically displayed on Fig. 6a. The obtained coil current Ic (α)

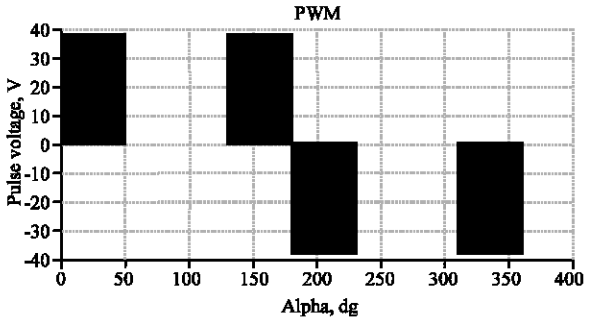


Fig. 5: Phase voltage of coil S3

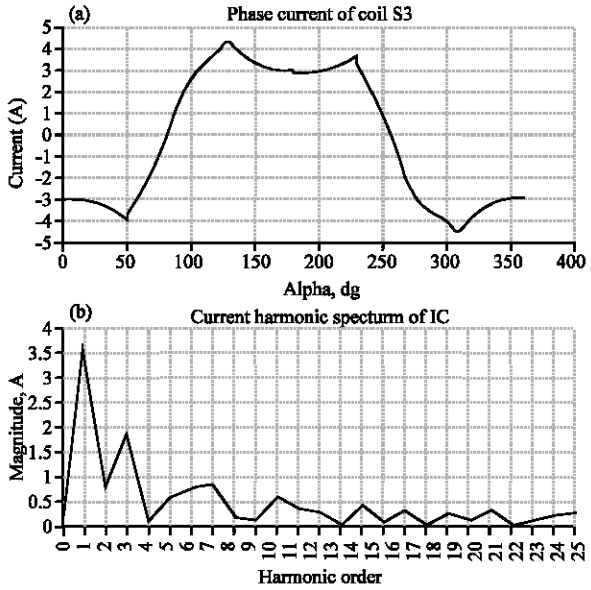


Fig. 6a: Phase current of S3 at certain speed ; and b) Current harmonic spectrum.

can be expressed in Fourier series by applying the FFT procedure, where the obtained results are displayed on Fig. 6b:

$$ic(\alpha) = \sum_{\nu=1}^{\infty} Im\nu.\sin(\alpha - \psi\nu) \tag{8}$$

**Electromagnetic torque:** The developed electromagnetic torque in the motor is produced by the following approaches:

**Asymmetrical rotor construction:** The developed torque consists of two components[1-4], reluctance torque Tr and electromagnetic torque Te. These torques are going to be called " original " in the present study.

**The reluctance torque:** This torque is independent of the motor excitation and depends on the permance in the airgap..

The permance in the airgap varied periodically with the rotor position, being maximum at the axis of the stator poles. Consider the rotor construction as shown on Fig.1, the reluctance torque is calculated using the coenergy method as follow:

$$T_{RA} = \frac{dW_{RA}(\alpha)}{d\alpha} = \frac{1}{2} F_{SA} \frac{dG(\alpha)}{d\alpha}$$
$$F_{SA} = N_{phA}.i_A(\alpha).K_{wA} \quad (9)$$
$$G(\alpha) = G_0 + \sum_{g=2,4}^{\infty} G_{mg}.\cos(g.N_t.\alpha - \beta_g)$$

The final expression of the reluctance torque for 2nd and 4th permance harmonics is:

$$T_{RA} = F_{SA}^2.\left(G_2 \sin(2\alpha - \beta_2) + 2G_4 \sin(4\alpha - \beta_4)\right) \quad (10)$$

The obtained reluctance torque expression indicates that null points torque occurs at $\alpha \neq 90, 180°$,, which is a good indicator for realizing self starting torque.

**The electromagnetic torque:** This component is obtained due to the interaction between the stator coil current and the rotor magnets, where the mathematical expression can be presented as follow[7-9]:

$$T_{EA} = \frac{dW_{EA}(\alpha)}{d\alpha} = F_{SA}.\phi_m(\alpha)$$
where: (11)
$$\phi_m(\alpha) = \int_{-\pi/2}^{\pi/2} F_m.\cos\alpha.G(\alpha)$$

is the produced rotor flux in the airgap, which depends on the magnetic permance and rotor MMF. The mathematical expressed as follow:

$$\phi_m(\alpha) = F_m.A\cos\alpha + F_m.B\sin\alpha$$
where:
$$A = 2G_0 + \frac{2}{3}G_2\cos 2\beta_2 - \frac{2}{15}G_4\cos 4\beta_4 \quad (12)$$
$$B = \frac{4}{3}G_2\sin 2\beta_2 - \frac{8}{15}G_4\sin 4\beta_4$$
$$F_m = L_m.H_m$$

The final expression for the electromagnetic torque for one coil S1 or S2 is:

$$T_{EA} = F_{SA}.A(F_m\sin\alpha - F_m\cos\alpha) \quad (13)$$

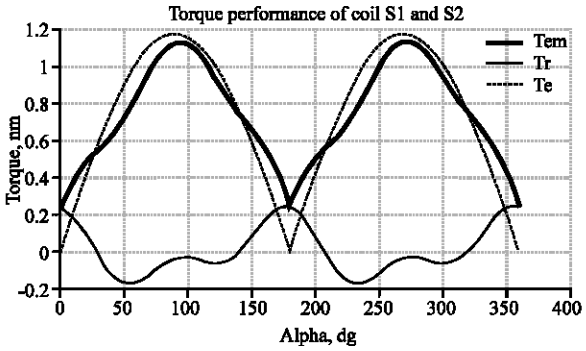


Fig. 7: Total Electromagnetic torque of coils S1 and S2.

The total motor torque presents the sum of both torques taking into account Eq. (10) and (13), has an expression expressed in Eq. (14), with graphically results illustrated on Fig.7 for certain speed, where it clearly shows that the motor achieved self starting condition.

$$T_{TA} = T_{RA} + T_{EA} \quad (14)$$

At the same time the generated torque ripples are relatively high, (which is the main drawback of this design). These ripples could be reduced extremely by applying the combination control method, where the produced torque is described hereinafter.

**Combination control:** This method is concentrated in producing additional torque by third coil S3 and have a purpose to eliminate the null regions of the original torque. Further more, the produced torque will play a significant role in ripples reduction overall the speed range, average torque increasing. As a result of this procedure achieving more speed stability with minimized fluctuations, which is important criteria for electrical drive technology. The torque expression is presented as follow:

$$T_{TC}(\alpha) = \frac{dW_{EC}(\alpha)}{d\alpha},$$
where: (15)
$$W_{EC}(\alpha) = \frac{1}{2}F_{SC}(\alpha,\varepsilon)^2.G(\alpha) + F_{SC}(\alpha,\varepsilon).\phi_m(\alpha)$$

The stator MMF produced by the third coil S3 with current Ic ($\alpha$) flow through the distributed winding in the stator periphery has space time variation with stepped character and minimized space-time ripples. Writing the trigonometrically terms as sums and difference leads to the following expression:

$$Fsc(\alpha,\varepsilon)=\frac{N_{phC}.Im1}{\pi}\sum_{\nu=1..}^{\infty}\sum_{\gamma=1..}^{\infty}\frac{Kvi.Kw\gamma}{\gamma}$$
$$\left[X(\nu,\gamma).\cos(\nu\alpha-\gamma\varepsilon)+Y(\nu,\gamma).\cos(\nu\alpha+\gamma\varepsilon)\right]$$

where:

$$X(\nu,\gamma)=1+\cos(\nu-\gamma)\frac{\pi}{2},\qquad Y(\nu,\gamma)=1+\cos(\nu+\gamma)\frac{\pi}{2},\qquad Kvi=\frac{Im\,\nu}{Im1}. \tag{16}$$

Since the coil current Ic ($\alpha$) depends on the rotor position and induced back emf, the electromagnetic torque produced by this coil TTC changes alternatively. This means that in some regions this torque will added to the original torque and subtracted in another regions. As a result of this adding and subtraction procedure, the produced total electromagnetic torque is expected to be with reduced ripples.

Hereinafter mathematical expression explaining the dependency of TTC on a few parameters, taking into account Eq. 15 and 16, the torque expression:

$$T_{TC}=T_{EC1}+T_{EC2}+T_{EC3}+T_{EC4}$$

where:

$$T_{EC1}=Fsc(\alpha,\varepsilon).G(\alpha)\frac{dFsc(\alpha,\varepsilon)}{d\alpha}$$
$$T_{EC2}=\frac{1}{2}Fsc(\alpha,\varepsilon)^2\frac{dG(\alpha)}{d\alpha} \tag{17}$$
$$T_{EC3}=Fsc(\alpha,\varepsilon)\frac{d\phi m(\alpha)}{d\alpha}$$
$$T_{EC4}=\phi m(\alpha)\frac{dFsc(\alpha,\varepsilon)}{d\alpha}$$

The obtained torque components of Eq. 17 are graphically displayed on Fig. 8. at the same conditions, where this torque has rich harmonic spectrum when acts alone, but will improve the total motor torque when acts together with the original torque.

The total torque produced by three coils is the sum of Eq. 14 and 17 as follow:

$$T_{EM}=T_{TA}+T_{TC} \tag{18}$$

The torque results are graphically displayed on Fig. 9a. for certain motor speed and the torque harmonic spectrum is displayed on Fig.9b. From the displayed results, it is shown that the put up tasks have been achieved.

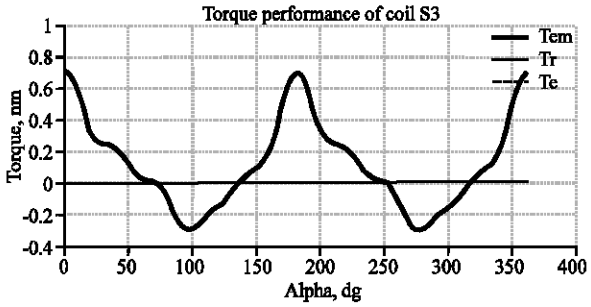


Fig. 8: Total electromagnetic torque of S3

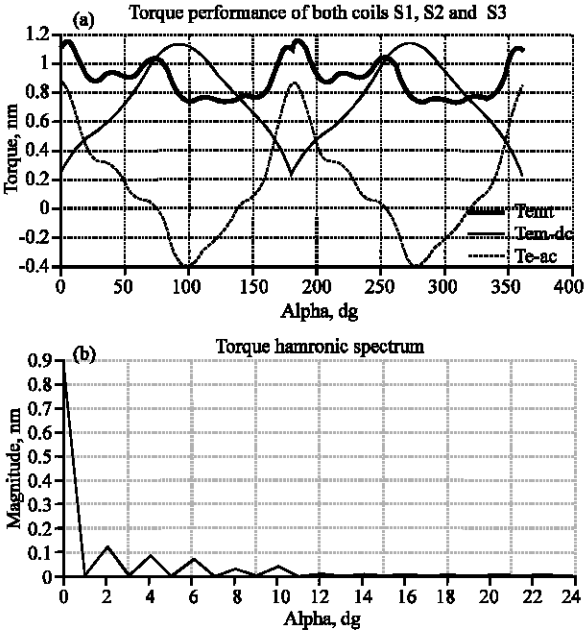


Fig. 9a: The total electromagnetic torque of both coils S1, S2 and S3; b) The torque harmonic spectrum.

## RESULTS

Referring to the motor design parameters listed in Table 1 and to the rotor design listed in the appendix, the discussed results in previous section can be supported with additional parameters[9-11] as follow:

**Torque Current ratio:** This parameter presents the ratio of the obtained mean torque to the root-mean square current:

$$TCR=\frac{T_{AV}}{I_{TRMS}}$$

Where

$$TAV=\frac{1}{T}\int_{0}^{T}T_{EM}(\alpha)d\alpha \tag{19}$$
$$I_{TRMS}=\sqrt{\sum_{\nu=1..}^{\infty}(I_{RMS\nu})^2}$$

Table 1: The motor parameters

| | | |
|---|---|---|
| Phase voltage | Vs, V | 38 |
| The induced counter voltage in coil S1 | EmA, V | 33 |
| The phase resistance of coils S1 and s2 | RA, Ω | 0.3 |
| The phase resistance of coil S3 | RC, Ω | 8.5 |
| The number of conductors of S1 and s2, | NphA | 60 |
| The number of conductors of S3, | NphC | 80 |
| The pole pairs | P | 2 |
| The induced voltage frequency | f1, Hz | 50 |
| The modulation frequency | fm, kHz | 20 |
| The rotor outside diameter | D, mm | 53 |
| The number of stator slots/pole | S,-- | 4 |
| The Magnet type: NdFeBr | | ---- |
| The permanent magnet depth, | hm, mm | 7 |
| The permanent magnet length, | Lm, mm | 60 |
| The permanent magnet width, | bm, mm | 5 |
| The permanent magnet density, | Bm, T | 0.6 |
| The stator active length | Lδ, mm | 60 |
| The permanent magnet coercive force (intensity) | Hm, kA/m | 40 |
| The active uniform air gap width | δ, mm | 0.5 |

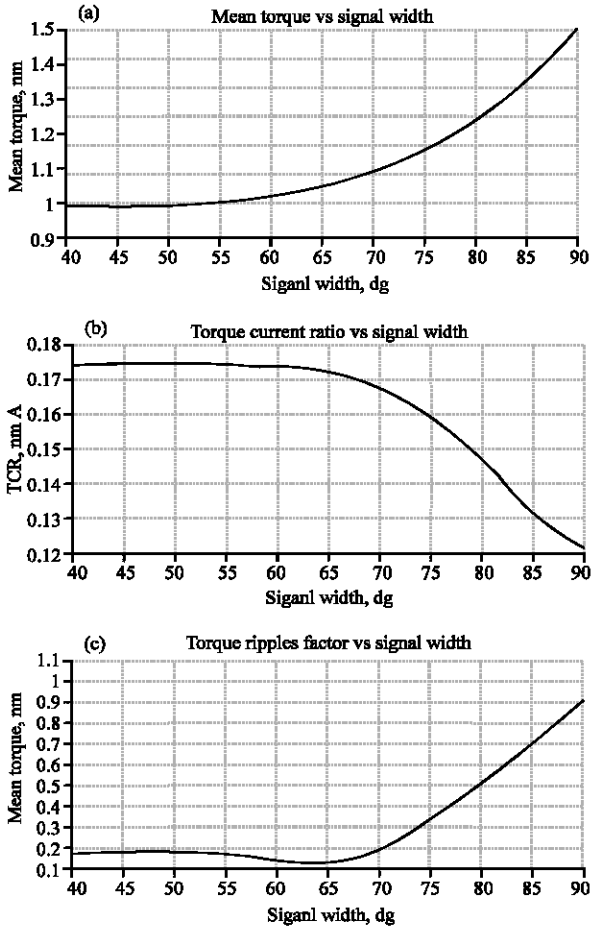


Fig. 10a: Motor mean torque ; b)Torque-current ratio; and Torque ripples factor versus signal width β

**Torque ripples factor:** This parameter presents the ratio of the torque ripples to motor mean torque:

$$TRF = \frac{T_R}{T_{AV}}$$

where: (20)

$$T_R = \sqrt{T^{-1}\int_0^T (T_{EM} - T_{AV})^2}$$

**Current harmonics factor:** This parameter presents the ratio of total rms current to the fundamental:

$$HFI = \sqrt{\left(\frac{I_{TRMS}}{I_{RMS}}\right)^2 - 1} \quad (21)$$

The width of control signal β Fig. 3b could be varied, where the obtained results are graphically illustrated on Fig. 10. From these results, it is clear shown that the motor mean (average) torque is significantly raised by increasing β, but this occurs on the expense of torque-current ratio, which decreases especially at certain value of β>65°. Furthermore the torque ripples factor is minimized at β = 65°, while the current harmonic factor is at it's maximum value. This means that the pulse- width must satisfy two contradict requirements high TCR and relatively low HFI.

## CONCLUSION

- The applied innovative design of two phase/three coils brushless DC motor with combined control produced electromagnetic torque realized self-starting and reduced fluctuation. This is due to the asymmetry in the rotor construction where the reluctance torque nulls occurs at different instants of the electromagnetic torque.
- By introducing the PWM control strategy for the third coil, the torque ripples decreases significantly due to the generated train of pulses with variable width. Once the torque ripples decreases, the motor speed will be more stable, with reduced power dissipation and increasing utility. The electromagnetic performances of the motor directly depends on the width of the PWM signal β.
- There is an optimized value of the main rotor slot's width, at which the motor draws a minimized current and significantly acceptable mean torque. The obtained value of slot's width should be applied as designed value for the motor prototype .
- The proposed design allows two operation modes depending on the required operation conditions with respect to the torque quality:

**First mode:** Three coils must energized with appropriate switching, therefore constant and stable torque with somewhat reduced mean torque, minimized ripples and fluctuations are obtained.

**Second mode:** Two coils S1 and S2 are to be energized, therefore the acceptable mean torque with significant ripples and fluctuation are obtained in the motor.

The described constructive modifications have certain advantages and disadvantages associated with the additional switching looses, vibration and noises, which mean's that choosing the required construction must take these parameters into consideration.

## ACKNOWLEDGMENT

The author would like to thank the League of Arab Universities for their financial support.

## REFERENCES

1. Alexander, K. and S.M. Peeran, 1987. Brushless DC motor using usymmetrical Field magnetization, In Proc. IA, pp: 319.
2. Kenjo, T. and S. Nagamori, 1985. Permanent-magnet and brushless dc motors, Oxford, England, Clarendon press.
3. Bolton, H.R. and R.A. Ashen, 1984. Influence of Motor Design and Feed-current Waveform on Torque Ripple in Brushless Dc Motor, IEE proc., pp; 82-90.
4. Faiz, J. and J.W. Finch, 1993. Aspects of design optimization for switched reluctance motors, IEEE Trans. On Energy Conversion 8, 1993, No.4, pp: 704.
5. Krimm, T.W., 1984. Harmonic control to reduce torque pulsations in brushless DC motor drives, MSEE Thesis, University of Kentucky.
6. Stephen, C., 1998. Electric Machines Fundamentals, 3rd Edn., McGraw-Hill International Edition.
7. Piriou, F., A. Razek, R. Perret and H. LeHuy, 1986. Torque Characteristics of Brsuhless DC Motor with Imposed Current Waveform, IEEE IAS Annual Meeting Conference Record.
8. Liber, F., J. Soulard and J. Engstrom, 2002. Design of a 4-pole line Start Permanent Magnet Synchronous Motor, Proceedings of ICEM. Bruge, Belgein.
9. Cros, J. and P. Viargue, 2002. Synthesis of high performance PM motors with concentrated windings, IEEE transactions on Energy Conversion, 17: 2.
10. Sameer, H.K., 2001. Implementation of an accurate mathematical method for modeling electromagnetic processes of brushless DC motor, MESM'2001, Amman. Jordan, pp: 31-38.
11. Libert, F. and J. Soulard, 2003. Design of a Direct-Driven Surface Mounted Permanent Magnet Motor for Low Speed Applications, Electric Machines and Drives Conference, IEMDC'03. IEEE International.